

Succinct Interaction-Aware Explanations

Sascha Xu, Joscha Cüppers, Jilles Vreeken

CISPA Helmholtz Center for Information Security
Saarbrücken, Germany
{sascha.xu, joscha.cueppers, vreeken}@cispa.de

Abstract

SHAP is a popular approach to explain black-box models by revealing the importance of individual features. As it ignores feature interactions, SHAP explanations can be confusing up to misleading. NSHAP, on the other hand, reports the additive importance for all subsets of features. While this does include all interacting sets of features, it also leads to an exponentially sized, difficult to interpret explanation. In this paper, we propose to combine the best of these two worlds, by partitioning the features into parts that significantly interact, and use these parts to compose a succinct, interpretable, additive explanation. We derive a criterion by which to measure the representativeness of such a partition for a model's behavior, traded off against the complexity of the resulting explanation. To efficiently find the best partition out of super-exponentially many, we show how to prune sub-optimal solutions using a statistical test, which not only improves runtime but also helps to detect spurious interactions. Experiments on synthetic and real world data show that our explanations are both more accurate resp. more easily interpretable than those of SHAP and NSHAP.

1 Introduction

Decision processes must be fair and transparent regardless of whether it is driven by a human or an algorithm. Post-hoc explainability methods offer a solution as they can generate explanations that are independent of the underlying model f , and are hence also applicable to powerful black-box machine learning models. One of the most popular post-hoc approaches is SHAP (Lundberg & Lee, 2017), which provides intuitive explanations for a decision $f(x)$ of an arbitrary model f for an individual x in terms of how much a specific input value x_i contributes to the outcome $f(x)$. Addi-

tive explanations over *single features* are succinct and easily understandable, but, only reliable when the underlying model is indeed additive. Whenever there are interactions between features in the model this can lead to misleading results (Gosiewska & Biecek, 2019).

Interaction index explanations (Lundberg et al., 2020; Sundararajan et al., 2020; Tsai et al., 2023) address this weakness by considering *groups of features* x_S with a non-additive effect on the prediction $f(x)$. NSHAP (Bordt & von Luxburg, 2023) is a recent interaction-based approach that decomposes a prediction $f(x)$ into a generalized additive model $\sum_{S \subseteq [d]} \Phi_S^n$, where each combination of features, of which there are exponentially many, is assigned an additive contribution. Although this permits modeling any interaction, the size of the explanation makes it arduous to compute, and even harder to interpret and make use of.

To illustrate, we show the explanations of SHAP, NSHAP, and our method, iSHAP for a bike rental prediction. On the left of Fig. 1 we give the explanation that SHAP provides. It is easy to understand, but counterintuitive: winter and humidity are listed as beneficial, while medium temperature is identified as a negative factor for bike rentals. On the right, we show the NSHAP explanation for all 1024 subsets of features. The simplicity of SHAP is exchanged for an overflow of detail; for example, **Temperature** has now equally strong positive and negative n^{th} order interactions and it is hard to say which are truly important. In fact, behind the visually appealing explanation there is a total of 751 non-zero NSHAP values to be considered.

In the middle, we show our proposed iSHAP explanation. It partitions the feature set into parts that significantly interact, and provides an additive explanation over these. iSHAP immediately reveals that there are two interactions responsible for the high predicted demand: it is a dry and relatively warm day for winter (**Season:4**, **Hum:0.49** and **Temp:0.39**) and a Saturday with little wind (**Weekday:6** and **Windspeed:0.15**).

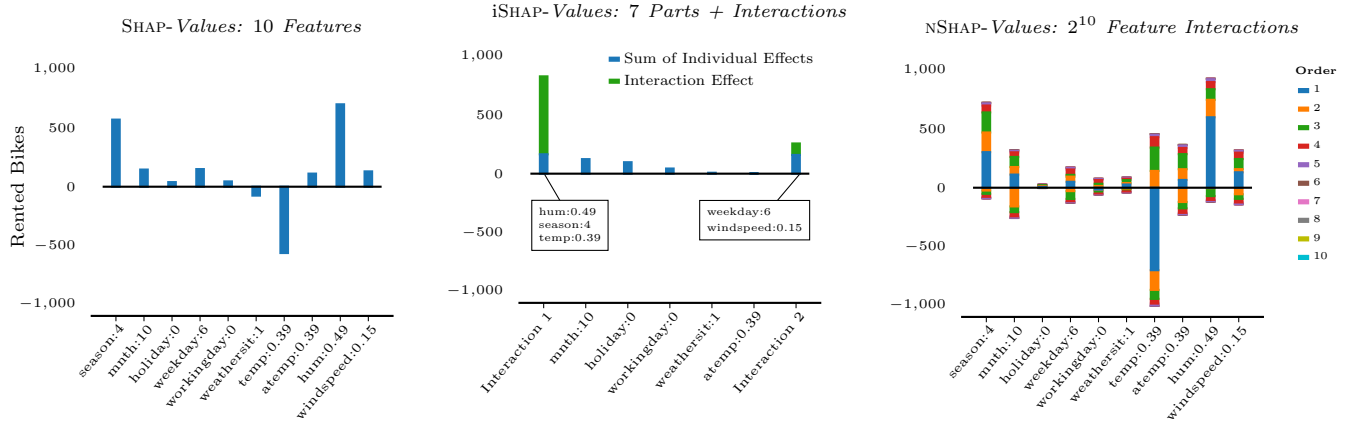


Figure 1: Comparison of SHAP (left), our approach iSHAP (middle) and NSHAP (right) on the Bike Sharing dataset (Fanaee-T & Gama, 2013). SHAP does not inform about any interactions, while NSHAP overflows with information. iSHAP provides a concise explanation for the high predicted demand: its is a warm and dry day for winter (**Season:4**, **Hum:0.49** and **Temp:0.39**) and a Saturday with little wind (**Weekday:6** and **Windspeed:0.15**).

In the following, we outline the theory and algorithm behind iSHAP to combine the best of both worlds: we propose to partition the feature set into parts that interact strongly, and use them to compose an interpretable, additive explanation. We formalize this by deriving an objective function for the ideal partition of an additive explanation. The objective is inspired by game theory and seeks to find those coalitions of players, which together best approximate the full game as an additive function. The main hurdle is on the computational side due to the combinatorial explosion of the number of possible partitions. To this end, we devise a statistical test to prune the search space by testing pairwise for significant interactions. We then show how to construct an additive explanation from the partition, and test them on various benchmarks against both additive and interaction based explanations.

2 Theory

We consider a machine learning model $f : \mathcal{X} \rightarrow \mathbb{R}$ with a domain \mathcal{X} over d univariate random variables X_1 to X_d . We denote a subset of input variables by X_S , where S is the index set and denote the set of all indices as $[d] = \{1, \dots, d\}$. We define an explanation as a set of tuples $\{(S_i, e_i)\}$ where S_i is an index set with an explanatory value e_i to the prediction $f(x)$. For example, SHAP explains using singletons $S_i = \{i\}$, where e_i are the Shapley values. NSHAP on the other hand uses all sets $S_i \subset [d]$ from the power set of features.

We view the local prediction $f(x)$ as a coalition game, where a set of players x_S receive a payoff $v(S)$

defined by a value function $v : 2^d \rightarrow \mathbb{R}$, which we then analyze to determine the contribution of each coalition, made up of individual features, to the prediction. W.l.o.g. we assume that the value function is normalized, i.e. $v(\emptyset) = 0$, which can be achieved by pre-processing f so that $E[f(X)] = 0$. In the context of machine learning, two main variants of value functions are used: the observational value function $v(S; f, x) = E[f(X)|X_S = x_S]$ (Lundberg & Lee, 2017), and the interventional value function $v(S; f, x) = E[f(X)|do(X_S = x_S)]$ (Janzing et al., 2020). Our method is based directly on v , which can then be instantiated with either distribution. In the following, we omit the specific instance of f and x and refer to the value function simply as $v(S)$.

2.1 Objective

Our goal is to construct an explanation $\{(S_i, e_i)\}$ for $f(x)$ that has a succinct and thus interpretable amount of components S_i , and where the additive interpretation $\sum_i e_i$ approximates the behavior of f best. For example, if f is a linear model, then the value function of a single feature i is the weight w_i times the deviation from the mean, i.e. $v(i) = w_i(x_i - E[X_i])$, and the value function of a coalition of features S is the sum of the individual value functions $v(S) = \sum_{i \in S} v(i)$. For complex models such as neural networks however, there exists no exact analytic decomposition in practice.

Instead, we focus on finding a partition Π of the features space $[d]$ such that each feature i is contained in only one set S_j . Each feature $i \in S_j$ is associated with only one explanatory value e_j , whilst still

informing about interactions between features in S_j . In particular, we want to find that partition Π that $\min (f(x) - \sum_{S \in \Pi} v(S))^2$, i.e. the partition Π that *approximates* f of x best. The general idea is that if feature x_i and x_j interact and have a large joint effect on the result, the local surrogate model will make a large mistake if x_i and x_j are not in the same set S .

It is easy to see that the objective is trivially minimized by $\Pi = \{[d]\}$, which would not give any insight into the inner workings of the model. Therefore, we regularize the complexity of the explanation by penalizing the number of allowed interactions through the $L0$ norm. For each set $S \in \Pi$, there are $|S||S - 1|/2$ pairwise interactions, making the full $L0$ norm of a partition $\mathcal{R}(\Pi) = \sum_{S \in \Pi} |S||S - 1|/2$. Thus, we define the optimal partition Π^* in regards to the value function v of an algorithmic decision $f(x)$ as the partition Π which minimizes

$$\begin{aligned} \Pi^* = \arg \min_{\Pi} & \left(f(x) - \sum_{S_i \in \Pi} v(S_i) \right)^2 \\ & + \lambda \cdot \sum_{S_i \in \Pi} \frac{1}{2} |S_i| |S_i - 1| \quad . \end{aligned} \quad (1)$$

The explanation $\{(S_i, e_i)\}$ is then constructed from the sets $S_i \in \Pi^*$ of the optimal partition.

2.2 Partitioning

Objective (1) poses a challenging optimization problem. Finding the best partition is a constrained variant of the subset sum problem and thus NP-hard (see Supplement A). The number of partitions for a set of d features is the Bell number B_d that grows super-exponentially with d , ruling out exhaustive search. Approximate solutions for subset sum problems can be computed in pseudo-polynomial time (Pisinger, 1999), they however require the value function to be computed for all elements of the power set, of which there are exponentially many.

Instead, our approach initially looks at all pairs of variables x_i and x_j , and seeks to determine whether they have an interactive, non-additive effect on the prediction $f(x)$. If there is no interaction, we can rule out the combination of x_i and x_j in the optimal partition, and thus prune the search space drastically.

Definition 1 *Given a value function v , the interaction \mathcal{I} between x_i and x_j in the context of x_S is defined as*

$$\mathcal{I}(i, j, S) = v(S \cup i) + v(S \cup j) - v(S \cup \{i, j\}) - v(S) .$$

This definition of interaction, as introduced in Lundberg et al. (2020), measures the effect of setting $X_i = x_i$ and $X_j = x_j$ individually, in contrast to the combined effect, whilst accounting for a covariate set x_S . We now show, that if for any covariate set S , there is no interaction between x_i and x_j , then i and j are not be grouped in the optimal partition with regard to Objective (1). To this end, we begin by showing that the additivity of effects for a pair x_i and x_j is a sufficient criterion to rule out their pairing, and then show in which cases we can use the absence of interaction as an indicator for additivity.

Theorem 1 *Let v be additive for the variables x_i and x_j , so that for all covariates $S \subseteq [d] \setminus \{i, j\}$ there exists a partition $A \cup B = S$ with*

$$v(A \cup i) + v(B \cup j) = v(S \cup \{i, j\}) .$$

Then, x_i and x_j do not occur together in the optimal partition Π^ in regards to Objective (1), i.e.*

$$\nexists S_k \in \Pi^* : i \in S_k \wedge j \in S_k .$$

Proof: *Assume the optimal partition Π^* contains a set S where $i, j \in S$. Then, the value function $v(S)$ is decomposable into $v(S) = v(A \cup i) + v(B \cup j)$. Thus, we may construct a partition Π' with $A \cup i$ and $B \cup j$, where the reconstruction error $f(x) - \sum_{S_i \in \Pi'} v(S_i)$ remains the same and its regularization penalty shrinks, i.e. $R(\Pi^*) > R(\Pi')$. It follows that the overall the objective of the partition Π' is lower than Π^* , contradicting its optimality. \square*

Theorem 1 confirms the intuition that if v is additive for two variables x_i and x_j , then they do not occur as part of the same set in the optimal partition. The main challenge lies in the exponential quantity of contexts S to consider, where the effect of x_i and x_j may differ, which is the same underlying problem hampering the interpretability and computability of nSHAP. Instead, we show how to reduce this effort to only a single test per pair x_i and x_j , which under some mild assumption allows to detect an absence of interaction and hence rule out their pairing from the optimal solution. The resulting explanations are tractable in real time and more comprehensible due to less overall components.

Assumption 1 *If v is additive for a partition A, B of S , i.e. $v(S) = v(A) + v(B)$, then it is also additive for all subsets $A' \subseteq A, B' \subseteq B$, so that*

$$\forall A' \subseteq A, B' \subseteq B : v(A') + v(B') = v(A' \cup B') .$$

Assumption 1 requires that the additivity of two sets of features A and B is preserved for all of their subsets. For example, if we find that $v(\{x_1, x_2, x_3\}) =$

$v(\{x_1, x_2\}) + v(\{x_3\})$, then we also assume that $v(\{x_1, x_3\}) = v(\{x_1\}) + v(\{x_3\})$. This holds for many popular value functions, including the interventional value function by Janzing et al. (2020) and the original observational value function used by Lundberg & Lee (2017) in conjunction with an underlying additive function f , but does not generally hold for Asymmetric Shapley Values (Frye et al., 2020) (see Supplement C).

Theorem 2 *If the expected interaction of a pair of variables i and j is not zero, i.e.*

$$E_S [\mathcal{I}(i, j, S)] \neq 0 ,$$

then v is not additive for i and j , i.e.

$$\begin{aligned} \exists S \subseteq [d] \setminus \{i, j\} : \forall A, B, A \cup B = S, A \cap B = \emptyset : \\ v(A \cup i) + v(B \cup j) \neq v(S \cup i, j) . \end{aligned}$$

Proof: *If there is interaction between i and j , we show that there exists a covariate set S for which v is not additive for i and j . First, we note that*

$$\begin{aligned} E_S [\mathcal{I}(i, j, S)] \neq 0 \\ \implies \exists S \subseteq [d] \setminus \{i, j\} : \mathcal{I}(i, j, S) \neq 0 , \end{aligned}$$

i.e. there exists a covariate set S for which the interaction is not zero. For this set S , it holds that

$$v(S \cup i) + v(S \cup j) \neq v(S \cup i, j) + v(S) . \quad (2)$$

If v indeed was additive for i and j , then for S there exists a partition $A \cup B = S$ so that

$$v(S \cup i, j) = v(A \cup i) + v(B \cup j) .$$

By Assumption 1, we know that this decomposition also holds for S , $S \cup i$ and $S \cup j$, so that we can rewrite Equation (2) as

$$\begin{aligned} v(A \cup i) + v(B) + v(A) + v(B \cup j) \\ \neq v(A \cup i) + v(B \cup j) + v(A) + v(B) . \end{aligned}$$

This statement is a contradiction, and thus proves that v is not additive for i and j . \square

With Theorem 2, we show that we can reject the additivity of a pair of variables i and j if their interaction is non-zero. As per Theorem 1, any pair of variables i and j that is additive is not grouped together in the optimal partition. Thus, to obtain the optimal partition Π^* , we need to only consider all interacting pairs of variables i and j .

Considering these pairs alone however does not suffice. Let i and j be non-additive, and let j and k be non-additive too, then we can show that i and k are also non-additive, i.e. potentially grouped together in the optimal partition.

Theorem 3 *Let v be non-additive for i and j , i.e.*

$$\begin{aligned} \exists S_1 \subseteq [d] \setminus \{i, j\} : \forall A, B, A \cup B = S_1, A \cap B = \emptyset : \\ v(A \cup i) + v(B \cup j) \neq v(S_1 \cup i, j) \end{aligned}$$

and let v be non-additive for j and k , i.e. $\exists S_2 \subseteq [d] \setminus \{j, k\} : \forall A, B : v(A \cup j) + v(B \cup k) \neq v(S_2 \cup j, k)$. Then v is also not additive for the variables i and k .

We provide the full proof in the Supplement B. Theorem 3 allows us to reject the additivity of a pair of variables i and j if they are connected by a path of interactions. This helps us to reduce the search space so that the partition contains only those sets where all variables are interconnected. In practice, we run the risk of falsely eliminating pairs of variables where their effect is inconclusive, i.e. the interaction is zero, and there is no path between them. Our evaluation however indicates that requiring significant interactions has a profusely positive effect by preventing the fit spurious interactions, whilst allowing the majority of true interactions to go through.

2.3 Explanation

Once the optimal partition Π^* is obtained, we use the discovered interacting sets $S_i \in \Pi^*$ as building blocks to explain the algorithmic decision $f(x)$. We set the contribution e_i of each feature set S_i to the Shapley values of a new game v' , where the players are made up by the sets S_i instead. This new game v' allows to only include either all or no features of a feature set S_i , and takes the values of the original value function v . As a result, we return for each algorithmic decision $f(x)$ based on the optimal partition an additive explanation $\{(S_i, e_i)\}_{S_i \in \Pi^*}$, where $\sum_i e_i = f(x)$. Finally, we quantify the amount of interaction in S_i using Definition 1 and extend it onto sets as the difference between their joint contribution and the contribution of grouped features individually $v(S_i) - \sum_{j \in S_i} v(j)$.

3 Algorithm

The number of possible partitions of a set of d variables is the Bell number, B_d . The total amount grows super-exponentially with the number of variables d , making it vital to restrict the search space. To this end, we introduce the iSHAP algorithm for Interaction-Aware Shapley Value Explanations. It enables us to find the optimal partition Π^* which minimizes the regularized reconstruction error of Objective 1.

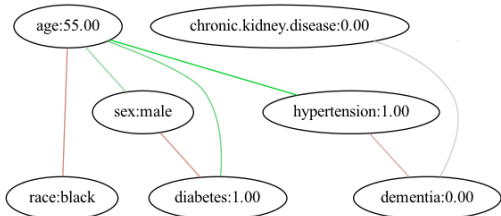


Figure 2: Interaction graph for predicted survival of a hospitalized COVID-19 patient. The detrimental effect of diabetes and hypertension on survival is alleviated by the relatively young age (55) of the patient.

3.1 Pairwise Interaction Test

Before we can find the optimal partition, we first identify all pairs of variables that show significant interaction. As per Theorem 2, for a pair x_i and x_j , we formulate the null-hypothesis of no interaction as

$$H_0 : E_S [\mathcal{I}(i, j, S)] = 0 .$$

We use a t -test to find statistically significant interaction effects under a user specified significance level α . We construct an undirected graph with a node for each feature, and draw an edge wherever H_0 is rejected. Figure 2 shows an example of such an interaction graph. Overall, the graph provides insight into the significant interactions which occur in the model and supplements the additive iSHAP explanation. With it, we can now run a much accelerated graph partitioning algorithm to find the best partitioning.

By Theorem 3, we know that any pair of nodes which is connected by a path in the interaction graph is not additive. Therefore, the optimal partition consists only of connected components of the interaction graph, and their subsets. This because for any pair of variables i and j which are not connected by a path, and therefore not additive, a partition Π which contains both i and j is suboptimal as per Theorem 1.

3.2 Search

Given the interaction graph we can derive all valid candidate partitions. A partition is valid if for each component S and all pairwise features $x_i, x_j \in S$ there exist a path between x_i and x_j in the interaction graph. In the naive exhaustive approach we test all valid partitions, and select the one which minimizes our objective. We evaluate all eligible partitions Π by sampling the value function $v(S)$ for each subset of features $S \in \Pi$, computing the reconstruction error $f(x) - \sum_{S \in \Pi} v(S)$ and add the regularization penalty $\mathcal{R}(\Pi)$. To avoid re-

computing the value function for the same subset in different partitions, we additionally buffer the value function $v(S)$ for re-use in other partitions. iSHAP-Exact does an exact search over all eligible candidates and is guaranteed to find the optimal partition, but comes to its limit for many variables, for which we introduce a greedy search variant. iSHAP-Greedy is a bottom up approach, which starts with the all singleton partition $\Pi_0 = \{S_1 = \{x_1\}, \dots, S_d = \{x_d\}\}$. Iteratively, the two sets S_i and S_j which yield the highest gain in the objective are merged. Here, only merges are considered which do not violate the interaction graph, i.e. S_i and S_j are connected by an path. Naturally, the greedy approach is not guaranteed to be optimal, but as we will see in the evaluation, achieves near optimal results in practice. The pseudocode for both the greedy and exact variant and a complexity analysis can be found in the Supplement D.

4 Related Work

We focus on post-hoc, model-agnostic explainability approaches (Ribeiro et al., 2016b) that treat the model f as a black-box and generate explanations by perturbing the input and analyzing the output. Here, explanations can be categorized into global explanations of f and local explanations of a particular decision $f(x)$.

Friedman (2001) introduced the partial dependence plot (PD), a global explanation method that visualizes the relationship between a variable X_i and the predicted output $f(X)$. PD plots are well suited for an injective relationship between X_i and $f(X)$, however, unlike our method, are not well suited for cases where interaction effects between more than two variables occur. Functional ANOVA (analysis of variance) (Hooker, 2004, 2007) is another global explanation approach which aims at discovering non-additive interactions between input variables. Sivill & Flach (2023) propose to discover interacting feature sets for a given model, one step further Herbringer et al. (2023) aim to partition the feature space into subspaces by minimizing feature interactions. Overall, global model explanations can give a good overview over a model f , but produce non-conclusive explanations when faced with complex, highly interactive functions where it is hard to create a single global summary.

Local explanations on the other hand aim to explain the decision of a model $f(x)$ for a particular instance x . Local Interpretable Model Agnostic Explanations (LIME) (Ribeiro et al., 2016a), is perhaps the most influential post-hoc explainability method. LIME explains a prediction $f(x)$ by constructing a local surrogate model f' that is interpretable, for example a

Linear Regression or a Decision Tree. LIME is model agnostic and generates simple, intuitive explanations, but has a fuzzy data sampling process and no guarantees as it is based on purely heuristics. As LIME fits a local model, the resulting explanations can be misleading (Ribeiro et al., 2018) or non informative for cases where x is *far* from any decision boundary.

A different style of explanation are approaches which explain a decision $f(x)$ through combinations of features x_i (Carter et al., 2019; Ribeiro et al., 2018). In essence both method find a sufficient set of variables such that the prediction $f(x)$ does not change. In contrast to our method they can not provide explanations for regression models and they do not explain which combinations of variables has which effect on the prediction. Counterfactual explanations (Wachter et al., 2017; Karimi et al., 2020; Van Looveren & Klaise, 2021; Mothilal et al., 2020; Poyiadzi et al., 2020) are another type of local explanations that bring together causality and explainability. Algorithmic Recourse (Joshi et al., 2019; Karimi et al., 2021) goes one step further and wants to find the best set of changes to reverse a models decision. These methods are most appropriate if the user seeks actionable insights, i.e. how to reverse a decision, and, in contrast, do not explain a prediction.

One of the most widely used approaches for explainable AI are Shapley values (Lundberg & Lee, 2017). Shapley values where originally introduced (Shapley, 1953) in game theory to measure the contributions of individual players. Recently different variants have been proposed like asymmetric Frye et al. (2020) and causal Shapley values (Heskes et al., 2020). Unlike our method they provide per feature attributions and no further insight into which features interact. Describing interaction is getting more attention in recent years. Jung et al. (2022) propose to quantify the effect of a group of causes through *do*-interventions, but focus on estimating those effects from non-experimental data. Jullum et al. (2021) propose to compute Shapley values on predefined feature sets, where they suggest to either group semantically related features or correlated features. Unlike our approach the feature sets are not discovered and independent of the model.

Most closely related is a recent class of so called *interaction index* explanations. The work by Lundberg et al. (2020) introduces *SHAP interaction values* extending SHAP explanations to all pairwise interactions. Sundararajan et al. (2020) and Tsai et al. (2023) both derive Shapley interaction indices for binary features that cover the entire powerset. Most recently nSHAP was introduced (Bordt & von Luxburg, 2023), which extends Shapley interaction values to sets of degree n . Similar to our method, nSHAP explains a decision

$f(x)$ through a generalized additive model $\sum_{S \subseteq [d]} \Phi_S^n$. The main difference is that nSHAP provides a value for the entire powerset of features, whereas our method chooses a succinct representation selecting interacting components.

5 Experiments

In this section we empirically evaluate iSHAP. We compare to SHAP (Lundberg & Lee, 2017) and LIME (Ribeiro et al., 2016a), the most widely used additive explanation methods, and nSHAP (Bordt & von Luxburg, 2023). We implemented iSHAP in Python, and used the original Python implementation of SHAP, nSHAP and LIME. We provide the code and data generators in the Supplement. All experiments were conducted on a consumer-grade laptop.

5.1 Discovering Interactions

First, we examine whether iSHAP recovers truly interacting sets of variables, and compare it against nSHAP, which also informs about interactions. To this end, we generate random generalized additive models f (GAMs) for which we can define ground truth sets of interacting features S_i . We sample d feature variables X_j from a uniform or a Gaussian distribution. Then, we construct the ground truth partition Π by repeatedly sampling sets S_i of arbitrary size from a Poisson distribution. Next, we define f as $f(x; \Pi) = \sum_{S_i \in \Pi} f_i(X_{S_i})$, with a non-additive inner function f_i . For the full details on the experimental setup we refer to Supplement E.

Given a GAM $f(x; \Pi)$, we now compute for a random data point the iSHAP and the nSHAP explanation and evaluate the obtained feature partition $\hat{\Pi}$ (for nSHAP, we take those sets with the highest interaction value). We measure the quality of the predicted partition $\hat{\Pi}$ compared to the ground truth Π using the *F1* score between the sets $S_i \in \Pi$ and $\hat{S}_i \in \hat{\Pi}$. Additionally, we evaluate whether an explanation finds interactions on a pairwise level, where we compute the *F1*-score on paired variables $j, k \in S_i$ and $j', k' \in \hat{S}_i$.

We show the performance of iSHAP-Greedy, iSHAP-Exact and nSHAP in Fig. 3. For up to 10 variables, where nSHAP terminates within the time limit of 10 min/explanation, iSHAP is more accurate than nSHAP in detecting full sets of interactions. This advantage persists across all tested combinations of feature distributions $P(X)$ and classes of inner functions (Fig. 3 right). Notably, iSHAP-Greedy performs almost as good as iSHAP-Exact, showing the effectiveness of our

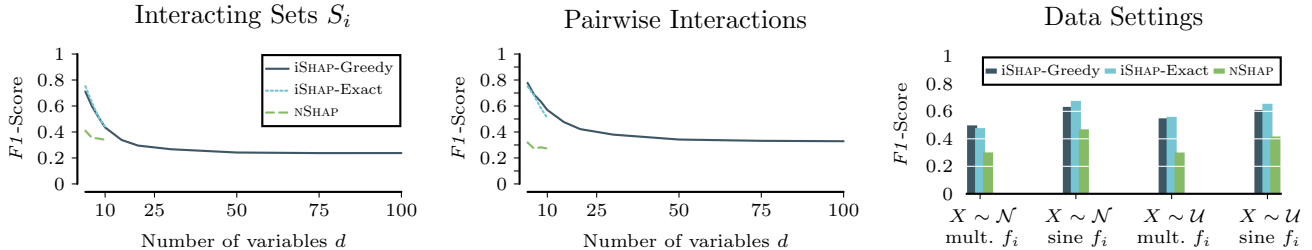


Figure 3: [Higher is better] $F1$ scores of recovered interactions in GAMs. iSHAP is more accurate than nSHAP in detecting full sets of interacting features (left) and pairwise interactions (middle), and can do so on more features. iSHAP-Greedy is equivalent to iSHAP-Exact and outperforms nSHAP across all data settings(right).

interaction test in restricting the search space. In Supplement F, we provide an ablation study showing how performance deteriorates without the interaction test.

In addition, we also evaluate the *pairwise interaction* $F1$ score, as for an increasing amount of variables, the accuracy over sets deteriorates. In particular, with ground truth (Age, Sex, Weight, Height), finding (Age, Sex, Weight) gives no score on a set level, but contains half of the pairwise interactions. We show the pairwise $F1$ score in the middle of Fig. 3. Here too, iSHAP strongly outperforms nSHAP and finds at least parts of the ground truth interacting sets, hence achieving a higher pairwise score. Overall, iSHAP-Greedy reliably uncovers most feature interactions and can do so given many variables.

5.2 Surrogate Model Accuracy

Next, we evaluate the accuracy of iSHAP, SHAP, nSHAP and LIME explanations as *surrogate models* to explain different classes of models. Given a model f , this evaluation as described by Poursabzi-Sangdeh et al. (2021) presents a user with a number of explanations and then asks him to predict the models output on new, unseen data. As all evaluated explanation methods have explicit, additive surrogate models, we can directly compute the models output as implied by the resp. explanation. To this end, given two datapoints $x^{(1)}$ and $x^{(2)}$, we firstly construct a new datapoint x' by taking features uniformly at random from $x^{(1)}$ or $x^{(2)}$. Then, for each feature, depending on which datapoint it came from, we add its explained additive contribution to obtain the implied $\hat{f}(x')$ and compute the MSE to the true prediction $f(x')$ (full detail in Supplement E).

We consider five regression and two classification datasets¹ with increasingly complex, non-additive

models f : linear models, support vector machines (SVM), random forests (RF), multi-layer perceptrons (MLP) and k-nearest neighbors (KNN). We report the R^2 between the true model outcome and that predicted by the surrogate model in Fig. 4.

For linear models f the additivity assumption holds fully, which is reflected in the near perfect accuracy of all methods. When using SVMs and random forests, the overall accuracy of all methods is decreased. Here, iSHAP emerges as the most accurate surrogate model with an R^2 over 0.9. LIME struggles to model the local decision surface of an MLP as a linear model, and nSHAP’s exponential amount of modeled interactions of nSHAP does not describe k-nearest neighbors models well. SHAP does not take into account any interactions, leaving iSHAP to consistently provide the most accurate surrogate model explanations.

From the performance across different datasets, shown in the middle of Fig. 4, we see that iSHAP outperforms SHAP, nSHAP and LIME on all datasets. In particular, we find that for the low-dimensional *Diabetes* and *Insurance* datasets, all methods perform well as surrogate models. On datasets with more features and interactions between these, such as the *Credit* dataset, we find that iSHAP achieves a R^2 score of 0.9, while SHAP, nSHAP and LIME are only reach an R^2 score of 0.6-0.7. On the *Life Expectancy*, *Student* and *Breast Cancer* datasets where SHAP and LIME struggle and nSHAP times out, iSHAP provides by far the best surrogate models. This increase in performance comes with an increased computational effort for iSHAP compared to the simpler SHAP and LIME. Still, in contrast to nSHAP’s limit of 16 features, iSHAP-Exact can explain up to 32 variables within an hour, and iSHAP-Greedy scales up to hundreds of features whilst informing about the most significant interactions (right of Fig. 4).

¹California (Pace & Barry, 1997), Diabetes (Pedregosa et al., 2011), Insurance (Lantz, 2019), Life (Rajarshi et al., 2019),

Student (Cortez & Silva, 2008), Breast Cancer (Dua & Graff, 2017) and Credit (Dua & Graff, 2017)

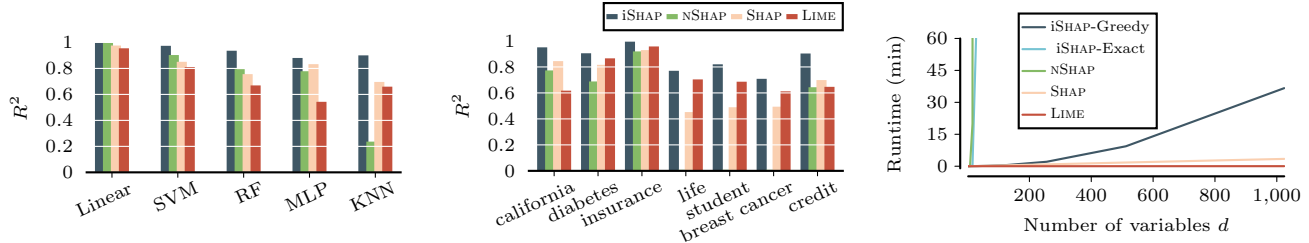


Figure 4: R^2 for surrogate models of iSHAP, nSHAP, SHAP and LIME across different model classes (left) and datasets (middle). iSHAP provides the most accurate surrogate model across all model classes and datasets, whilst scaling to more dimension than nSHAP (right).

5.3 Case Study: Covid-19 Patient

Finally, we conduct a qualitative comparison between the Shapley value based explanations provided by iSHAP, SHAP and nSHAP. For this, we consider a Covid-19 dataset containing survival data of 1,540 hospitalized patients (Lambert et al., 2022). We train a random forest classifier to predict the likelihood of patient survival, based on diverse biomarkers such as age and pre-existing conditions. For each patient we provide the respective iSHAP, SHAP and nSHAP explanation in the following anonymized repository². We show in Table 1 the SHAP (left), nSHAP (middle) and iSHAP (right) explanations for a patient which was hospitalized, and for which the model correctly predicted survival. We note that iSHAP-Greedy and SHAP explanations were computed within a second, whereas nSHAP took 30 mins.

We discuss the explanations in turn. The features that SHAP identifies as key to survival seem to be reasonable at first glance, but upon closer inspection are at least partly counterintuitive. **Hypertension:1** is marked as a positive factor and **Diabetes:1** as having only a slight negative effect, despite both are known risk factors for Covid-19 (Parveen et al., 2020). A very strong positive effect is attributed to **Age:55** even though there many much younger patients in the dataset.

To obtain further insight, we move on to the nSHAP explanation shown in the middle. We show the top 13 out of 2516 interaction coefficients, the actual values of which we provide in Supplement G. Like SHAP, nSHAP also identifies **Age** as a positive marginal factor, but additionally shows that it is included in many higher-order interacting sets, interacting with **Hypertension**, **Diabetes** and **Race** amongst others in various combinations. The amount of redundance and inconclusive values makes a clear interpretation of them hard, for ex-

ample (**Age**, **Hypertension**, **Diabetes**, **Race**) is given a contribution of -9% to survival chances, while (**Age**, **Hypertension**) alone improve odds by 7.8% supposedly. The same phenomenon occurs across the board and does not reveal which these interacting sets are, let alone which out of the 2516 we should focus on.

Thus, we inspect the iSHAP explanation shown on the right. It partitions the feature set into six parts, and unlike the competing explanations, clearly identifies there are two interacting factors contributing to survival: the **Age:55** in conjunction with **Hypertension:1** and **Diabetes:1**, as well as the absence of **Hyperlipidemia** and **Coronary Artery Disease**. The positive interaction of age with diabetes and hypertension is explained as follows. While diabetes and hypertension are negative marginal factors for survival across the entire data set, their effect is significantly reduced for a patient of only 55 years old compared to the on-average much older patients in the dataset. This is reflected in the strong positive interaction found by iSHAP, but also explains the high SHAP value of the feature **Age:55** as it is due to the *sum* of the marginal and the interaction effects. Second, we see that **Hyperlipidemia:0** and **Coronary Artery Disease:0** are positively interacting factors for survival. Coronary artery disease is known to be a risk factor for Covid-19 patients (Szarpak et al., 2022), and thus its absence is a positive factor for survival. Hyperlipidemia is strongly associated with coronary artery disease (Goldstein et al., 1973), thus its absence validates the **Coronary Artery Disease:0** feature and interacts as a positive factor for survival.

Overall, we see that all three explanations describe the same phenomena, but do so in different levels of detail and succinctness. The SHAP explanation is arguably the most compact, but also the least detailed as it cannot explain the interactions that are important to understand the underlying mechanisms. The nSHAP explanation is arguably the most detailed, but, also the hardest to interpret, as it lists all interaction

²<https://anonymous.4open.science/r/ICML-24-iSHAP-Case-Study-C439>

Feature	Effect (%)	Feature Set	Effect (%)	Feature Set	Effect (%)	Feature Set	Individual Effect+ Interaction Effect(%)
age:55	28.1	age	15.1	hypertension, diabetes	4.5	diabetes:1, age:55, hypertension:1	10.2 + 18.6
race:black	0.9	age, hypertension, race, dia- betes	-9.0	age, race, di- abetes, CAD	4.2	hyperlipidemia:0, CAD:0	4.5 + 1.9
sex:male	-0.1	age, hypertension	7.8	age,race	-4.1	sex	-3.5 + 0
hypertension:1	7.1	age, race, hypertension	7.5	age, hyper- lipidemia, CAD	3.6	race	4.0 + 0
hyperlipidemia:0	-0.2	age, race, diabetes	6.5			copd	0.2 + 0
diabetes:1	-3.6	age, diabetes	4.8			chf	0.0 + 0
CAD:0	7.3	diabetes	-4.7				
chf:0	0.0	CAD	4.7				
CeVD:0	0.0						

(a) SHAP values

(b) Top-k nSHAP values (2516 total)

(c) iSHAP values

Table 1: Shapley value-based explanations for predicted Covid-19 survival odds. In (a) we show feature-wise SHAP values, in (b) nSHAP values for all feature subsets, and in (c) iSHAP values, attributed to partitioned features.

coefficients. The iSHAP explanation offers the best of both worlds: it is as interpretable as SHAP, and includes the main interactions as found by nSHAP, so to succinctly explain the models decision and making the user aware of the most important interactions.

6 Conclusion

In this paper, we proposed a model agnostic, post-hoc explanation method. In contrast to existing explanations, we directly integrate significant interactions between sets of features x_{S_i} into a succinct, additive explanation. We showed how to use a statistical test to guaranteed find the underlying optimal partitioning of features and avoid fitting spurious interactions. Our algorithm iSHAP is an effective and fast procedure that takes the theoretical results into practice. On synthetic data we have shown that iSHAP returns accurate, ground truth interactions, and on real world data, we find that iSHAP is in general a more accurate surrogate model than the state-of-the-art.

For future work, we plan to extend iSHAP to allow multiple interactions per variable. Furthermore, we want to extend the definition of interaction to be able to differentiate between any distribution of interaction effects.

Impact Statement

In this paper we introduced iSHAP, a model agnostic approach to explain black-box model predictions. As our research focuses on providing understandable explanations, with the explicit goal of making the explanations interpretable our method can potentially be used to discover undesired/unfair interactions that occur in a black-box model. However, it is important to stress that our explanations do not make causal statements about the underlying data generating process,

especially when the explained model is trained on sensitive data such as census.

References

- Bordt, S. and von Luxburg, U. From shapley values to generalized additive models and back. In *International Conference on Artificial Intelligence and Statistics*, pp. 709–745. PMLR, 2023.
- Carter, B., Mueller, J., Jain, S., and Gifford, D. What made you do this? understanding black-box decisions with sufficient input subsets. In *Proceedings of the International Conference on Artificial Intelligence and Statistics (AISTATS)*, pp. 567–576. PMLR, 2019.
- Cortez, P. and Silva, A. M. G. Using data mining to predict secondary school student performance. 2008.
- Dua, D. and Graff, C. UCI machine learning repository, 2017. URL <http://archive.ics.uci.edu/ml>.
- Fanaee-T, H. and Gama, J. Event labeling combining ensemble detectors and background knowledge. *Progress in Artificial Intelligence*, pp. 1–15, 2013. ISSN 2192-6352. doi: 10.1007/s13748-013-0040-3. URL [WebLink].
- Friedman, J. H. Greedy function approximation: a gradient boosting machine. *The Annals of Statistics*, pp. 1189–1232, 2001.
- Frye, C., Rowat, C., and Feige, I. Asymmetric shapley values: incorporating causal knowledge into model-agnostic explainability. *Advances in Neural Information Processing Systems*, 33:1229–1239, 2020.
- Goldstein, J. L., Hazzard, W. R., Schrott, H. G., Bierman, E. L., Motulsky, A. G., et al. Hyperlipidemia in coronary heart disease i. lipid levels in 500 survivors of myocardial infarction. *The Journal of Clinical Investigation*, 52(7):1533–1543, 1973.

- Gosiewska, A. and Biecek, P. Do not trust additive explanations. *arXiv preprint arXiv:1903.11420*, 2019.
- Herbinger, J., Bischl, B., and Casalicchio, G. Decomposing global feature effects based on feature interactions. *arXiv preprint arXiv:2306.00541*, 2023.
- Heskes, T., Sijben, E., Bucur, I. G., and Claassen, T. Causal shapley values: Exploiting causal knowledge to explain individual predictions of complex models. *Advances in Neural Information Processing Systems*, 33:4778–4789, 2020.
- Hooker, G. Discovering additive structure in black box functions. In *Proceedings of the 10th ACM International Conference on Knowledge Discovery and Data Mining (SIGKDD)*, Seattle, WA, pp. 575–580, 2004.
- Hooker, G. Generalized functional anova diagnostics for high-dimensional functions of dependent variables. *Journal of Computational and Graphical Statistics*, 16(3):709–732, 2007.
- Janzing, D., Minorics, L., and Blöbaum, P. Feature relevance quantification in explainable ai: A causal problem. In *Proceedings of the International Conference on Artificial Intelligence and Statistics (AISTATS)*, pp. 2907–2916. PMLR, 2020.
- Joshi, S., Koyejo, O., Vijitbenjaronk, W., Kim, B., and Ghosh, J. Towards realistic individual recourse and actionable explanations in black-box decision making systems. *arXiv preprint arXiv:1907.09615*, 2019.
- Jullum, M., Redelmeier, A., and Aas, K. groupshapley: Efficient prediction explanation with shapley values for feature groups. *arXiv preprint arXiv:2106.12228*, 2021.
- Jung, Y., Kasiviswanathan, S., Tian, J., Janzing, D., Blöbaum, P., and Bareinboim, E. On measuring causal contributions via do-interventions. In *International Conference on Machine Learning*, pp. 10476–10501. PMLR, 2022.
- Karimi, A.-H., Barthe, G., Balle, B., and Valera, I. Model-agnostic counterfactual explanations for consequential decisions. In *International Conference on Artificial Intelligence and Statistics*, pp. 895–905. PMLR, 2020.
- Karimi, A.-H., Schölkopf, B., and Valera, I. Algorithmic recourse: from counterfactual explanations to interventions. In *Proceedings of the 2021 ACM conference on fairness, accountability, and transparency*, pp. 353–362, 2021.
- Lambert, B., Stopard, I. J., Momeni-Boroujeni, A., Mendoza, R., and Zuretti, A. Using patient biomarker time series to determine mortality risk in hospitalised covid-19 patients: a comparative analysis across two new york hospitals. *Plos one*, 17(8): e0272442, 2022.
- Lantz, B. *Machine learning with R: expert techniques for predictive modeling*. Packt publishing ltd, 2019.
- Lundberg, S. M. and Lee, S.-I. A unified approach to interpreting model predictions. *Advances in Neural Information Processing Systems*, 30, 2017.
- Lundberg, S. M., Erion, G., Chen, H., DeGrave, A., Prutkin, J. M., Nair, B., Katz, R., Himmelfarb, J., Bansal, N., and Lee, S.-I. From local explanations to global understanding with explainable ai for trees. *Nature machine intelligence*, 2(1):56–67, 2020.
- Mothilal, R. K., Sharma, A., and Tan, C. Explaining machine learning classifiers through diverse counterfactual explanations. In *Proceedings of the 2020 Conference on Fairness, Accountability, and Transparency*, pp. 607–617, 2020.
- Pace, R. K. and Barry, R. Sparse spatial autoregressions. *Statistics & Probability Letters*, 33(3):291–297, 1997.
- Parveen, R., Sehar, N., Bajpai, R., and Agarwal, N. B. Association of diabetes and hypertension with disease severity in covid-19 patients: A systematic literature review and exploratory meta-analysis. *Diabetes research and clinical practice*, 166:108295, 2020.
- Pedregosa et al. Scikit-learn: Machine learning in python, 2011. Dataset available at <https://scikit-learn.org/stable/datasets.html>.
- Pisinger, D. Linear time algorithms for knapsack problems with bounded weights. *Journal of Algorithms*, 33(1):1–14, 1999.
- Poursabzi-Sangdeh, F., Goldstein, D. G., Hofman, J. M., Wortman Vaughan, J. W., and Wallach, H. Manipulating and measuring model interpretability. In *Proceedings of the 2021 CHI conference on human factors in computing systems*, pp. 1–52, 2021.
- Poyiadzi, R., Sokol, K., Santos-Rodriguez, R., De Bie, T., and Flach, P. Face: feasible and actionable counterfactual explanations. In *Proceedings of the AAAI/ACM Conference on AI, Ethics, and Society*, pp. 344–350, 2020.

- Rajarshi, K., Russell, D., and Wang, D. Life expectancy (who). <https://www.kaggle.com/datasets/kumarajarshi/life-expectancy-who>, 2019. Kaggle: Online Data Science Community.
- Ribeiro, M. T., Singh, S., and Guestrin, C. "why should i trust you?" explaining the predictions of any classifier. In *Proceedings of the 22nd ACM International Conference on Knowledge Discovery and Data Mining (SIGKDD), San Francisco, CA*, pp. 1135–1144, 2016a.
- Ribeiro, M. T., Singh, S., and Guestrin, C. Model-Agnostic Interpretability of Machine Learning. In *ICML Workshop on Human Interpretability in Machine Learning (WHI)*, June 2016b.
- Ribeiro, M. T., Singh, S., and Guestrin, C. Anchors: High-precision model-agnostic explanations. In *Proceedings of the AAAI Conference on Artificial Intelligence*, volume 32, 2018.
- Shapley, L. S. A value for n-person games. In *Contributions to the Theory of Games (AM-28)*, pp. 307–317. Princeton University Press, 1953.
- Sivill, T. and Flach, P. Shapley sets: Feature attribution via recursive function decomposition. *arXiv preprint arXiv:2307.01777*, 2023.
- Sundararajan, M., Dhamdhere, K., and Agarwal, A. The shapley taylor interaction index. In *International conference on machine learning*, pp. 9259–9268. PMLR, 2020.
- Szarpak, L., Mierzejewska, M., Jurek, J., Kochanowska, A., Gasecka, A., Truszewski, Z., Pruc, M., Blek, N., Rafique, Z., Filipiak, K. J., et al. Effect of coronary artery disease on covid-19—prognosis and risk assessment: A systematic review and meta-analysis. *Biology*, 11(2):221, 2022.
- Tsai, C.-P., Yeh, C.-K., and Ravikumar, P. Faith-shap: The faithful shapley interaction index. *Journal of Machine Learning Research*, 24(94):1–42, 2023.
- Van Looveren, A. and Klaise, J. Interpretable counterfactual explanations guided by prototypes. In *Machine Learning and Knowledge Discovery in Databases. Research Track: European Conference, ECML PKDD 2021, Bilbao, Spain, September 13–17, 2021, Proceedings, Part II 21*, pp. 650–665. Springer, 2021.
- Wachter, S., Mittelstadt, B., and Russell, C. Counterfactual explanations without opening the black box: Automated decisions and the gdpr. *Harv. JL & Tech.*, 31:841, 2017.

A Problem Complexity

The Subset Sum Problem is defined as follows:

Input: Given a set of integers $A = \{a_1, a_2, \dots, a_n\}$ and a target integer t .

Output: Determine if there exists a subset $A' \subseteq A$ such that the sum of its elements is equal to t .

In our case, the set of integers A is the set of all possible values of the value function $v(S)$ for $S \subseteq [d]$, i.e. $A = \{v(\{1\}), v(\{1, 2\}), v(\{1, 2\}), \dots, v([d])\}$. The target integer t is the prediction $f(x) - \mu$. Note that we can transform any fixed precision floating point number into an integer by multiplying it with a sufficiently large constant. We impose additional constraints on a valid solution, namely that the set A' must be a partition of $[d]$. We are interested in the closest subset sum variant, where instead the objective is to minimize the difference between the sum of A' and t , i.e. the prediction error $f(x) - \mu$. Additionally, our objective contains a regularization term $\mathcal{R}(A')$ that penalizes the number of sets in the partition A' .

B Proofs

B.1 Proof of Theorem 1

Theorem 1 *Let v be additive for the variables x_i and x_j , so that for all covariates $S \subseteq [d] \setminus \{i, j\}$ there exists a partition $A \cup B = S$ with*

$$v(A \cup i) + v(B \cup j) = v(S \cup \{i, j\}).$$

Then, x_i and x_j do not occur together in the optimal partition Π^ in regards to Objective (1), i.e.*

$$\nexists S_k \in \Pi^* : i \in S_k \wedge j \in S_k.$$

Proof: *Assume the optimal partition Π^* contains a set S where $i, j \in S$. Then, the value function $v(S)$ is decomposable into*

$$v(S) = v(A \cup i) + v(B \cup j).$$

Thus, we may construct a partition Π' with $A \cup i$ and $B \cup j$. Let $E[f(X)] = 0$ (achievable by pre-processing), then the reconstruction error of Π' is

$$f(x) - \sum_{T' \in \Pi'} v(T') = \left(f(x) - \sum_{T \in \Pi^*} v(T) \right) - v(S) + v(A \cup i) + v(B \cup j).$$

As per the assumption, $v(S) = v(A \cup i) + v(B \cup j)$, so the reconstruction error of Π' is equal to the reconstruction error of Π^ . For the regularization penalty of the new partition elements $A' = A \cup i$ and $B' = B \cup j$ in Π' it holds that*

$$|A'|(|A'| - 1)/2 + |B'|(|B'| - 1)/2 < (|A'| + |B'|)(|A'| + |B'| - 1)/2,$$

which shows that it is smaller than the regularization penalty of Π^ for $S \cup i, j$. Thus, the overall objective of Π' is lower than Π^* , contradicting its optimality. ζ □*

Assumption 1 *If v is additive for a partition A, B of S , i.e. $v(S) = v(A) + v(B)$, then it is also additive for all subsets $A' \subseteq A, B' \subseteq B$, so that*

$$\forall A' \subseteq A, B' \subseteq B : v(A') + v(B') = v(A' \cup B').$$

B.2 Proof of Theorem 2

Proof: *If there is interaction between i and j , we show that there exists a covariate set S for which v is not additive for i and j . First, we note that*

$$\begin{aligned} & E_S [\mathcal{I}(i, j, S)] \neq 0 \\ \implies & \exists S \subseteq [d] \setminus \{i, j\} : \mathcal{I}(i, j, S) \neq 0, \end{aligned}$$

i.e. there exists a covariate set S for which the interaction is not zero. For this set S , it holds that

$$v(S \cup i) + v(S \cup j) \neq v(S \cup i, j) + v(S). \quad (3)$$

If v indeed was additive for i and j , then for S there exists a partition $A \cup B = S$ so that

$$v(S \cup i, j) = v(A \cup i) + v(B \cup j).$$

By Assumption 1, we know that this decomposition also holds for S , $S \cup i$ and $S \cup j$, so that we can rewrite Equation (3) as

$$\begin{aligned} & v(A \cup i) + v(B) + v(A) + v(B \cup j) \\ & \neq v(A \cup i) + v(B \cup j) + v(A) + v(B). \end{aligned}$$

This statement is a contradiction, and thus proves that v is not additive for i and j . \square

B.3 Proof of Theorem 3

Theorem 3 Let v be non-additive for i and j , i.e.

$$\begin{aligned} & \exists S_1 \subseteq [d] \setminus \{i, j\} : \forall A, B, A \cup B = S_1, A \cap B = \emptyset : \\ & v(A \cup i) + v(B \cup j) \neq v(S_1 \cup i, j) \end{aligned}$$

and let v be non-additive for j and k , i.e. $\exists S_2 \subseteq [d] \setminus \{j, k\} : \forall A, B : v(A \cup j) + v(B \cup k) \neq v(S_2 \cup j, k)$. Then v is also not additive for the variables i and k .

Proof: Assume that v is additive for i and k , i.e. $\forall S_3 \subseteq [d] \setminus \{i, k\} : \exists A, B : v(A \cup i) + v(B \cup k) = v(S_3 \cup i, k)$.

Now consider a set S_1 for which v is not additive in regards to i and j , i.e. $\forall A_1, B_1 : v(A_1 \cup i) + v(B_1 \cup j) \neq v(S_1 \cup i, j)$ and the set S_2 for j and k respectively. We construct a set $S_3 = (S_1 \cup S_2 \cup \{j\}) \setminus \{i, k\}$, for which v now has to be additive with regard to i and k , i.e. there exists a partition A_3, B_3 so that $v(A_3 \cup i) + v(B_3 \cup k) = v(S_3 \cup i, k)$.

There are two cases to consider, either $j \in A_3$ or $j \in B_3$. Let $j \in B_3$, then we can construct a new sub-partition $A_1 = S_1 \cap A_3$ and $B_1 = S_1 \cap (B_3 \cup k)$. A_1 and B_1 are subsets of $A_3 \cup i$ and $B_3 \cup k$, so that by Assumption 1 additivity is preserved for A_1 and B_1 . Therefore, it holds that $v(A_1 \cup i) + v((B_1 \setminus j) \cup j) = v(S_1 \cup i, j)$, since $A_1 \cup B_1 = S_1$ as $S_1 \subseteq S_3 \cup k$. This contradicts the assumption that v is non-additive for i and j .

Similarly, we can show that $j \in A_3$ violates the assumption that v is non-additive for j and k , and conclude that v must in fact be non-additive for i and k . In the interaction graph, this allows us to reject the additivity of a pair of variables i and j if they are connected by a path, and justifies the use of connected components over cliques as search space. \square

C Additivity of Value Functions

We consider two value functions: the observational value function

$$v(S; f, x) = \mathbb{E} [f(X) | X_S = x_S]$$

by Lundberg & Lee (2017), where it is assumed that all variables are independent of each other, i.e. $\forall i \neq j : X_i \perp\!\!\!\perp X_j$, and the interventional value function

$$v(S; f, x) = \mathbb{E} [f(X') | do(X'_S = x_S)]$$

by Janzing et al. (2020), where we consider as features variables the model inputs X'_i that are purely determined by the real world counterpart X_i . Hence, intervening on the model input as $do(X'_S = x_S)$ only has an effect on the input X'_S .

Let f now be additive for two sets A and B , so that $f(x) = g(x_A) + h(x_B)$, then the value function $v(A; f, x) + v(B; f, x)$ is transformed into

$$\begin{aligned} & \mathbb{E} [f(X)|X_A = x_A] + \mathbb{E} [f(X)|X_B = x_B] \\ &= \mathbb{E} [g(X)|X_A = x_A] + \mathbb{E} [h(X)|X_A = x_A] + \mathbb{E} [g(X)|X_B = x_B] + \mathbb{E} [h(X)|X_B = x_B] . \end{aligned}$$

We can drop the conditioning of $X_A = x_A$ where there is only h and vice versa for $X_B = x_B$ and g . This is possible both with the independence assumption in the observational Shapley values by Lundberg & Lee (2017), and the causal model as postulated by Janzing et al. (2020). This leaves us with

$$\mathbb{E} [g(X)|X_A = x_A] + \mathbb{E} [h(X)] + \mathbb{E} [g(X)] + \mathbb{E} [h(X)|X_B = x_B] = \mathbb{E} [g(X)|X_A = x_A] + \mathbb{E} [h(X)|X_B = x_B] + \mu .$$

By convention, we preprocess $f(X)$ so that $\mu = \mathbb{E} [f(X)] = 0$, and μ hence can be dropped. Now, we similarly decompose $v(S; f, x)$ as

$$\mathbb{E} [f(X)|X_S = x_S] = \mathbb{E} [g(X) + h(X)|X_S = x_S] = \mathbb{E} [g(X)|X_S = x_S] + \mathbb{E} [h(X)|X_S = x_S] .$$

Now we again drop X_B from g and X_A from h and are left with

$$\mathbb{E} [g(X)|X_A = x_A] + \mathbb{E} [h(X)|X_B = x_B] ,$$

which shows the additivity for any set A and B for which f is decomposable.

D Algorithm

iSHAP consists of two main subroutines: `find_interactions` and `find_partition`. The first subroutine is the same for both the greedy and the optimal algorithm. iSHAP-Greedy uses a greedy, bottom-up approach to find the best partition, while iSHAP-Exact uses an exhaustive search.

find_interactions. As input, `find_interactions` receives a data point x , a model f and a sample \hat{X} of $P(X)$. It returns all pairwise interactions between features that are statistically significant, encoded as a graph G . We initialize the interaction graph G with d nodes, where each node represents a single feature. We then sample n_s new data points $x^{(j)'}$ from the empiric data distribution, either marginally, conditionally or interventional as required by the value function v . For each data point $x^{(j)'}$, we sample a random intervention $z \in \{0, 1\}^d$ with $p = 0.5$. We then intervene on the i -th feature on the j -th data point $x^{(j)'}$, i.e. $x_i^{(j)'} = x_i$, if $z_i^{(j)} = 1$.

Now, for each pair of features i, j , we test the hypothesis

$$H_0 : \mathbb{E}_S [v(S \cup i) - v(S) + v(S \cup j) - v(S)] = \mathbb{E}_S [v(S \cup i, j) - v(S)]$$

by taking dividing up the sample $\{f(x^{(j)'})\}$ into four subsets according to the intervention $z^{(j)}$:

- $v(S \cup \{i, j\}) \leftarrow \{f(x^{(j)'})|i, j \in z^{(j)}\}$
- $v(S \cup \{i\}) \leftarrow \{f(x^{(j)'})|i \in z^{(j)}, j \notin z^{(j)}\}$
- $v(S \cup \{j\}) \leftarrow \{f(x^{(j)'})|j \in z^{(j)}, i \notin z^{(j)}\}$
- $v(S) \leftarrow \{f(x^{(j)'})|i, j \notin z^{(j)}\}$

Now, we can test the hypothesis using a two-sided t-test with significance level α with unequal variances, also known as Welch's t-test. If the hypothesis is rejected, we add an edge between the nodes i and j to the graph G . By splitting up the sample into four subsets, we can test the hypothesis for each pair of features i, j on the same sample, which is more efficient than testing each pair on a separate sample as it reduces the number of required samples and thus evaluations of f by the amount of pairwise interactions, i.e. $O(d^2)$.

Algorithm 1: find_interactions($f, x, \hat{X}, n_S, \alpha$)

Input: Data point x , model f , sample \hat{X} , number of samples n_S , significance level α

- 1 Initialize graph G with d nodes.
- 2 Sample n_S interventions $z^{(k)} \in \{0, 1\}^d$ with $p = 0.5$.
- 3 Sample n_S new points $x^{(k)'}$ from the marginal/conditional/interventional distribution using \hat{X} .
- 4 **for** $i = 1 : n_S, j = 1 : d$ **do**
- 5 **if** $z_j^{(i)} = 1$ **then**
- 6 Set the i -th feature on the j -th data point $x_i^{(j)'}$ to x_i
- 7 **for** $i = 1 : d, j = i + 1 : d$ **do**
- 8 Sample of $v(S \cup \{i, j\}) \leftarrow \{f(x^{(k)'}) | i, j \in z^{(k)}\}$
- 9 Sample of $v(S \cup \{i\}) \leftarrow \{f(x^{(k)'}) | i \in z^{(k)}, j \notin z^{(k)}\}$
- 10 Sample of $v(S \cup \{j\}) \leftarrow \{f(x^{(k)'}) | i \notin z^{(k)}, j \in z^{(k)}\}$
- 11 Sample of $v(S) \leftarrow \{f(x^{(k)'}) | i, j \notin z^{(k)}\}$
- 12 $p =$ Welch's t-test for $v(S \cup \{i\}) + v(S \cup \{j\}) = v(S \cup \{i, j\}) + v(S)$
- 13 **if** $p < \alpha$ **then**
- 14 Add edge (i, j) to G
- 15 **return** G

D.1 Complexity

The complexity of the greedy search is cubic. For a fully connected graph we have to evaluate $d(d-1)/2$ merges, where we can take at most d steps before arriving at the complete set $[d]$. In each step, we have to estimate the value function v with n samples, whose complexity we denote by $O(v(n, d))$. Hence, its complexity is $O(d^3)O(v(n, d))$.

find_partition. The find_partition subroutine takes in addition the graph G from find_interactions and uses the same data point x , the model f and the sample \hat{X} of $P(X)$. find_partition returns the best scored partition Π in regards to Objective 1.

For the greedy approach, we initialize Π with d singleton sets, i.e. $\Pi = \{S_i | S_i = \{i\}\}_{i=1}^d$. We merge all eligible pairs of sets $S_i, S_j \in \Pi$ into a new set $S_i \cup S_j$ and score the new partition Π' . Eligibility is given if the graph G contains an edge between an element of S_i and an element of S_j . Each step, we merge the pair of sets that yields the best score and terminate once no more improvement is possible.

The exhaustive approach is a brute-force search over all possible partitions Π . We restrict the search space by only considering partitions Π , where all elements $S_i \in \Pi$ are connected in the graph G . Then, we score each partition Π and return the best scored partition.

Algorithm 2: score_partition($\Pi, v, \lambda, f(x)$)

- 1 Pred $\leftarrow 0$
- 2 **for** $S_i \in \Pi$ **do**
- 3 Pred \leftarrow Pred + $v(S_i)$
- 4 Error \leftarrow Pred - $f(x)$
- 5 Reg $\leftarrow \lambda \cdot \sum_{S_i \in \Pi} |S_i|$
- 6 **return** Error + Reg

Explanation. Once we have found the best scored partition Π , we can explain the prediction $f(x)$ by computing the Shapley values for a new game v' which has as its players the elements of Π instead of the features $\{1, \dots, d\}$.

Algorithm 3: find_partition_greedy($G, v, f(x), \lambda$)

Input: Graph G , value function v , prediction $f(x)$, regularization parameter λ

- 1 $d \leftarrow$ number of nodes in G
- 2 Initialize $\Pi = \{S_i | S_i = \{i\}\}_{i=1}^d$.
- 3 **while** *True* **do**
- 4 Best Score \leftarrow score_partition($\Pi, v, \lambda, f(x)$)
- 5 Candidate Found \leftarrow False
- 6 **for** $S_i, S_j \in \Pi$ **do**
- 7 **if** $\exists k \in S_i, l \in S_j : (k, l) \in G$ **then**
- 8 Candidate $\Pi' \leftarrow \Pi$
- 9 $\Pi' \leftarrow \Pi' \cup \{S_i \cup S_j\} \setminus \{S_i, S_j\}$
- 10 Candidate Score = score_partition($\Pi', v, \lambda, f(x)$)
- 11 **if** *Candidate Score* < *Best Score* **then**
- 12 Best Score \leftarrow Candidate Score
- 13 $\Pi \leftarrow \Pi'$
- 14 Candidate Found \leftarrow True
- 15 **if** *Candidate Found* = *False* **then**
- 16 Break
- 17 **return** Π

Algorithm 4: find_partition_exhaustive($G, v, f(x), \lambda$)

Input: Graph G , value function v , prediction $f(x)$, regularization parameter λ

- 1 $d \leftarrow$ number of nodes in G
- 2 Best Score $\leftarrow \infty$
- 3 **for** Π *in all partitions of* $[d]$ **do**
- 4 **if** $\exists S_i, S_j \in \Pi : \nexists k \in S_i, l \in S_j : (k, l) \in G$ **then**
- 5 **continue**
- 6 Score \leftarrow score_partition($\Pi, v, \lambda, f(x)$)
- 7 **if** *Score* < *Best Score* **then**
- 8 Best Score \leftarrow Score
- 9 Best $\Pi \leftarrow \Pi$
- 10 **return** Best Π

Algorithm 5: iSHAP($f, x, \hat{X}, n_S, v, \alpha, \text{greedy}$)

Input: Data point x , model f , sample \hat{X} , number of samples n_S , value function v , significance level α

- 1 Interaction Graph $G \leftarrow$ find_interactions($f, x, \hat{X}, n_S, \alpha$)
- 2 **if** *greedy* **then**
- 3 Partition $\Pi \leftarrow$ find_partition_greedy($G, v, f(x), \lambda$)
- 4 **else**
- 5 Partition $\Pi \leftarrow$ find_partition_exhaustive($G, v, f(x), \lambda$)
- 6 Value function $v'(S)$ of game with Π as players, $v'(S) = v(S)$ if $S \in \mathcal{P}(\Pi)$
- 7 Compute Shapley values ϕ_i for $i = 1, \dots, m$ using $S_i \in \Pi$ as players using v'
- 8 **return** Explanation $\{(S_i, \phi_i)\}_{S_i \in \Pi}$, Interaction Graph G

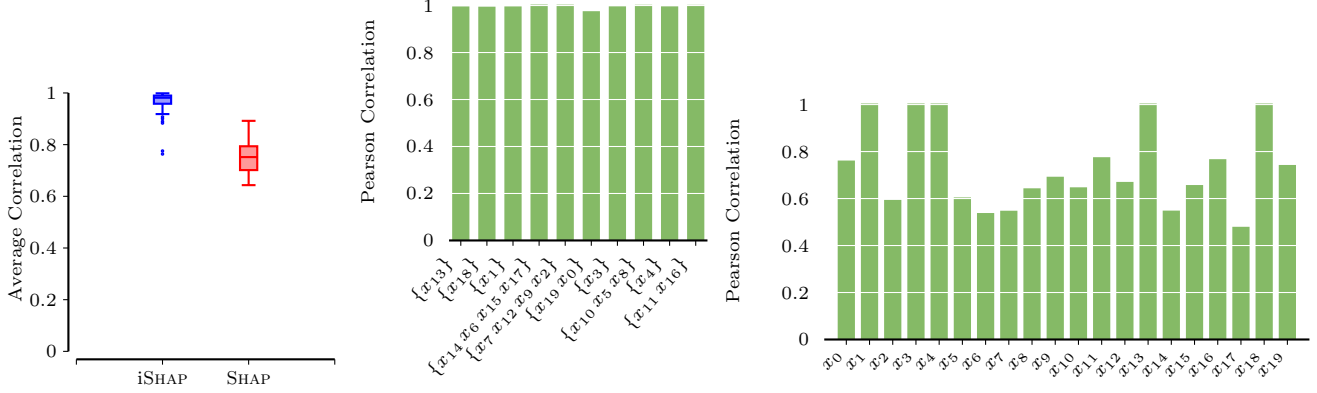


Figure 5: Comparison between ground truth feature importance (gradient times feature values) and the respective iSHAP values and SHAP values. On the left, we show the average correlation over all models. In the middle, we show the correlation between the iSHAP values and the ground truth for a specific model, on the right, we show the correlation between the ground truth and the SHAP values.

The value function v' is defined only for those sets S which are elements of the power set of Π . On that set, the value function v' is defined as $v'(S) = v(S)$ as the underlying model f is the same.

On this new game, we can compute the Shapley values ϕ_i for each element $S_i \in \Pi$. The Shapley value ϕ_i is the average marginal contribution of the element S_i to the value of the game v' . iSHAP returns the Shapley values ϕ_i as the explanation for the prediction $f(x)$, in addition to the interaction graph G and the partition Π .

E Experiments

E.1 Interaction Experiments

We first verify whether iSHAP accurately recovers the correct sets of variables for a generalized additive model. To this end, we generate a random function f over $d \in \{4, 6, 8, 10, 15, 20, 30, 50, 75, 100\}$ variables. To obtain a function with additive components, we partition the variables into sets S_i , where we iteratively sample the size of each set from a Poisson distribution with $\lambda = 1.5$, over which we define function $f(X) = \sum_{S_i \in \Pi} f_i(X_{S_i})$, whereas inner functions f_i we consider

- $f_i(X_{S_i}) = \prod_{j \in S_i} a_{i,j} \cdot X_j$, $a_{i,j} \in \pm[0.5, 1.5]$
- $f_i(X_{S_i}) = \sin\left(\sum_{j \in S_i} a_{i,j} \cdot X_j\right)$, $a_{i,j} \in \pm[0.5, 1.5]$

We sample all the underlying d variables either from a normal distribution: $P(X_j) = N(\mu, \sigma^2)$, $\mu \in [0, 3]$, $\sigma \in [0.5, 1.5]$ or a uniform distribution: $X_j \in \mathcal{U}(0, 3)$. In total, for we test the accuracy of 100 explanations for each combination of d , inner function and sampling distribution. Each time, we sample a random function f and dataset X of 10 000 points. We use the observational value function $v(S) = E[f(X)|X_S = x_S]$, where we sample X_i individually as they are independently generated. For a random $x \in X$, we generate the partition \hat{P} with iSHAP, using as significance level $\alpha = 0.01$ and as regularization coefficient $\lambda = 5e-3$.

Ground Truth Feature Importance Next, we evaluate whether the reported iSHAP values align with the ground truth feature importance, to this end, we first need to define the ground truth feature importance for sets of variables. For purely linear functions the importance of a single feature is $v(i, x', f) = w_i x'_i - w_i E[X_i]$, where w_i is the weight of feature i in f . We use the same concept for general additive models, where we use $f_i(X_{S_i}) = \prod_{j \in S_i} a_{i,j} \cdot X_j$, $a_{i,j} \in \pm[0.5, 1.5]$ as inner functions, hence the importance of a feature set S_i for a given sample is,

$$v(S_i, x', f) = \frac{\partial^{|S_i|} f}{\prod_{j \in S_i} \partial x_j} (x'_1, \dots, x'_d) * \prod_{j \in S_i} x'_j \quad .$$

Since the expected value is constant offset, we omit it. We compute person correlation between the iSHAP explanation and the ground truth $v(S_i, x', f)$.

We consider the same setup as described above, with $d = 20$, we generate 100 random models, for each model we uniform at random select 300 datapoints and generate the respective explanations. In Figure 5 (left) we show the average of the average correlation over all models. For comparison, we conduct the analog experiment, over the same set of models and datapoints, with SHAP values, computing the correlation between SHAP values and the respective partial derivative times the feature value. We observe a near-perfect correlation between ground truth and iSHAP values, while the SHAP values are less correlated with their respective gradients.

In Figure 5 (middle) we show the correlation between the individual additive components, for a specific model, and on the right the correlation of SHAP values with the respective gradient times feature values. While iSHAP gets near perfect correlation, SHAP gets a much lower correlation on average and only gets near near-perfect correlation for additive components that include only a single variable.

With this experiment, we show that iSHAP gives better insight into general additive models and models that can (locally) be approximated with GAM's.

E.2 Accuracy Experiments

We consider five regression and two classification dataset: *California* (Pace & Barry, 1997), *Diabetes* (Pedregosa et al., 2011), *Insurance* (Lantz, 2019), *Life* (Rajarshi et al., 2019), *Student* (Cortez & Silva, 2008) with increasingly complex, non-additive models f : linear models, support vector machines (SVM), random forests (RF), multi-layer perceptrons (MLP) and k-nearest neighbors (KNN). This experiment is for each dataset repeated 100 times and goes as follows: we pick two instances $x^{(1)}$ and $x^{(2)}$ from a dataset. We use these to construct a new data point x' by uniformly at random choosing the value for each variable X_i either as defined by $x^{(1)}$ or by $x^{(2)}$. Let I_1 be the indices of all feature values chosen from $x^{(1)}$, and I_2 from $x^{(2)}$. We run the respective explanation method for both $x^{(1)}$ and $x^{(2)}$. We can now use these additive explanations to obtain the prediction of the surrogate model for x' defined as By design, this scheme is not applicable for all random instances with partitions $\Pi^{(k)}$ and $\Pi^{(l)}$, in which case simply resample until we have an admissible input. We compute the implied prediction for the new data point x' in the following way for each method:

- iSHAP: $f(x') = \sum_{S_i \in \Pi_1, S_i \subseteq I_1} e_i^{(1)} + \sum_{S_j \in \Pi_2, S_j \subseteq I_2} e_j^{(2)}$
- SHAP: $f(x') = \sum_{i \in I_1} \phi_i^{(1)} + \sum_{j \in I_2} \phi_j^{(2)}$
- nSHAP: $f(x') = \sum_{S \subseteq I_1} \Phi_S^{(1)} + \sum_{S \subseteq I_2} \Phi_S^{(2)}$
- LIME: For each datapoint we obtain a surrogate model \hat{f}_1 and \hat{f}_2 . We take $\hat{f}_1(x')$ and $\hat{f}_2(x')$ and use whichever is closer to $f(x')$.

F Ablation Study

We seek to determine how iSHAP between the interaction test, or whether a simple, greedy merging algorithm alone already suffices. To this end, we perform an ablation study of iSHAP with and without interaction testing on the same synthetic data, both for the iSHAP-Greedy and iSHAP-Exact search. We use the same parameters as in the previous section. When ablation the interaction test, we simply skip the interaction test and use a fully connected interaction graph G instead.

We observe an average reduction of **53%** in runtime for the greedy search and by **95%** for the full search. This can be explained the reduction in search space, because over 99% less value functions need to be computed as well as 99% less partitions for the exhaustive search. This gain is partially offset by the interaction test, which introduces an overhead that grows quadratically with the number of variables, but is asymptotically offset by the exponential amount of value functions/ super-exponential amount of partitions. Finally, we compare the average $F1$ score with interaction testing against without. The interaction test improves the $F1$ score by **47%** for the greedy search and **20%** for the full search. This shows that the interaction test is crucial to obtain accurate explanations, especially for the greedy search.

G nShap Values Table for Bike Sharing and Covid-19 Explanations

We show an excerpt of the nSHAP values for the bike sharing in Table 6 and Covid-19 examples in Table 7. The full tables are available in csv format in the Supplementary Material.

Features	nSHAP-Value
season	302.7828
mnth	111.7951
holiday	7.2007
weekday	50.3631
workingday	-15.9047
weathersit	27.2326
temp	-702.0405
atemp	66.1923
hum	599.7396
windspeed	131.4193
season,mnth	40.7386
season,holiday	2.5113
season,weekday	-18.4194
season,workingday	6.8548
season,weathersit	4.2753
season,temp	259.2300
season,atemp	-23.0112
season,hum	21.3243
season,windspeed	-6.3036
mnth,holiday	-0.3594
mnth,weekday	5.2526
mnth,workingday	0.5199
mnth,weathersit	-2.7754
mnth,temp	-152.8421
mnth,atemp	-121.6957
mnth,hum	82.2086
mnth,windspeed	-40.7565
holiday,weekday	-0.7652
holiday,workingday	0.0000
holiday,weathersit	0.1169
holiday,temp	3.6589
holiday,atemp	0.9588
holiday,hum	1.7385
holiday,windspeed	0.2851
weekday,workingday	-2.1685
weekday,weathersit	-1.8315
weekday,temp	-34.5923
weekday,atemp	19.7831
weekday,hum	21.2906
weekday,windspeed	41.6146
workingday,weathersit	-2.6172
workingday,temp	14.5155
workingday,atemp	3.6907
workingday,hum	3.6916
workingday,windspeed	0.2563
weathersit,temp	8.4976
weathersit,atemp	7.8339
weathersit,hum	4.9372
weathersit,windspeed	-6.9062
temp,atemp	-91.1640
temp,hum	-6.8569
temp,windspeed	-50.0217
atemp,hum	150.6599

...

Features	nSHAP-Value
hum,windspeed	11.1615
season,mnth,holiday	-0.2216
season,mnth,weekday	-8.5839
season,mnth,workingday	-1.2126
season,mnth,weathersit	0.1137
season,mnth,temp	42.7639
season,mnth,atemp	38.2775
season,mnth,hum	-3.5914
season,mnth,windspeed	8.0619
season,holiday,weekday	-0.8984
season,holiday,workingday	-0.0000
season,holiday,weathersit	0.1893
season,holiday,temp	7.0437
season,holiday,atemp	5.8868
season,holiday,hum	2.0526
season,holiday,windspeed	0.9675
season,weekday,workingday	2.0534
season,weekday,weathersit	2.4728
season,weekday,temp	-46.6645
season,weekday,atemp	-0.3705
season,weekday,hum	-13.4172
season,weekday,windspeed	8.8701
season,workingday,weathersit	0.1749
season,workingday,temp	1.3530
season,workingday,atemp	1.3596
season,workingday,hum	-5.6364
season,workingday,windspeed	5.1050
season,weathersit,temp	11.4899
season,weathersit,atemp	1.5036
season,weathersit,hum	2.9810
season,weathersit,windspeed	3.7620
season,temp,atemp	140.3305
season,temp,hum	149.0698
season,temp,windspeed	48.0171
season,atemp,hum	11.7357
season,atemp,windspeed	-3.3548
season,hum,windspeed	16.7539
mnth,holiday,weekday	0.0344
mnth,holiday,workingday	0.0000
mnth,holiday,weathersit	0.0155
mnth,holiday,temp	-0.0307
mnth,holiday,atemp	-0.0113
mnth,holiday,hum	0.4018
mnth,holiday,windspeed	-0.0232
mnth,weekday,workingday	-1.5872
mnth,weekday,weathersit	-0.1717
mnth,weekday,temp	-9.1911
mnth,weekday,atemp	-1.2006
mnth,weekday,hum	-20.5531
mnth,weekday,windspeed	-16.6118
mnth,workingday,weathersit	-0.3498
mnth,workingday,temp	2.0001
mnth,workingday,atemp	6.3547

...

Figure 6: nSHAP values for bike sharing prediction.

Features	nSHAP-Value	Features	nSHAP-Value
age	0.1514	sex,chronic.kidney.disease	0.0013
race	0.0263	sex,asthma	0.0009
sex	-0.0434	sex,copd	0.0002
hypertension	-0.0034	sex,dementia	0.0040
hyperlipidemia	-0.0067	sex,cancer	0.0011
diabetes	-0.0473	hypertension,hyperlipidemia	-0.0009
coronary.artery.disease	0.0467	hypertension,diabetes	0.0454
chf	-0.0069	hypertension,coronary.artery.disease	-0.0009
cerebrovascular.disease	0.0043	hypertension,chf	0.0021
hepatitis	0.0019	hypertension,cerebrovascular.disease	0.0012
endstage.renal.disease	-0.0014	hypertension,hepatitis	0.0012
chronic.kidney.disease	0.0005	hypertension,endstage.renal.disease	0.0005
asthma	-0.0024	hypertension,chronic.kidney.disease	-0.0002
copd	-0.0025	hypertension,asthma	0.0001
dementia	0.0024	hypertension,copd	0.0018
cancer	0.0061	hypertension,dementia	-0.0045
age,race	-0.0407	hypertension,cancer	-0.0004
age,sex	0.0219	hyperlipidemia,diabetes	0.0024
age,hypertension	0.0781	hyperlipidemia,coronary.artery.disease	0.0106
age,hyperlipidemia	0.0016	hyperlipidemia,chf	-0.0023
age,diabetes	0.0483	hyperlipidemia,cerebrovascular.disease	0.0006
age,coronary.artery.disease	-0.0144	hyperlipidemia,hepatitis	-0.0004
age,chf	0.0155	hyperlipidemia,endstage.renal.disease	0.0004
age,cerebrovascular.disease	0.0016	hyperlipidemia,chronic.kidney.disease	-0.0018
age,hepatitis	-0.0005	hyperlipidemia,asthma	0.0016
age,endstage.renal.disease	0.0017	hyperlipidemia,copd	0.0013
age,chronic.kidney.disease	0.0013	hyperlipidemia,dementia	-0.0015
age,asthma	0.0023	hyperlipidemia,cancer	0.0011
age,copd	0.0061	diabetes,coronary.artery.disease	-0.0050
age,dementia	0.0083	diabetes,chf	-0.0082
age,cancer	0.0046	diabetes,cerebrovascular.disease	-0.0019
race,sex	0.0026	diabetes,hepatitis	0.0001
race,hypertension	-0.0330	diabetes,endstage.renal.disease	0.0001
race,hyperlipidemia	0.0010	diabetes,chronic.kidney.disease	-0.0025
race,diabetes	-0.0216	diabetes,asthma	-0.0006
race,coronary.artery.disease	-0.0109	diabetes,copd	0.0002
race,chf	0.0058	diabetes,dementia	-0.0021
race,cerebrovascular.disease	0.0029	diabetes,cancer	0.0009
race,hepatitis	-0.0002	coronary.artery.disease,chf	0.0101
race,endstage.renal.disease	0.0000	coronary.artery.disease,cerebrovascular.disease	0.0012
race,chronic.kidney.disease	-0.0001	coronary.artery.disease,hepatitis	0.0006
race,asthma	0.0009	coronary.artery.disease,endstage.renal.disease	0.0005
race,copd	0.0031	coronary.artery.disease,chronic.kidney.disease	0.0029
race,dementia	0.0023	coronary.artery.disease,asthma	0.0016
race,cancer	0.0010	coronary.artery.disease,copd	0.0029
sex,hypertension	0.0142	coronary.artery.disease,dementia	-0.0015
sex,hyperlipidemia	-0.0019	coronary.artery.disease,cancer	0.0029
sex,diabetes	-0.0267	chf,cerebrovascular.disease	-0.0006
sex,coronary.artery.disease	-0.0030	chf,hepatitis	-0.0002
sex,chf	-0.0027	chf,endstage.renal.disease	-0.0003
sex,cerebrovascular.disease	-0.0017	chf,chronic.kidney.disease	-0.0018
sex,hepatitis	-0.0004	chf,asthma	-0.0007

Figure 7: nSHAP values for covid-19 survival prediction.